ORGANOMETALLICS

Article

pubs.acs.org/Organometallics

Modification of [8,8,8-(H)(PPh$_3$)$_2$-9-(Py)-*nido*-8,7-RhSB$_9$H$_9$], Py = NC$_5$H$_5$, with Monodentate Phosphines: Reactivity and Mechanistic Insights

Beatriz Calvo,[†] Álvaro Álvarez,[†] Ramón Macías,*[,†] Pilar García-Orduña,[†] Fernando J. Lahoz,[†] and Luis A. Oro[†,‡]

[†]Instituto de Síntesis Química y Catálisis Homogénea (ISQCH), Universidad de Zaragoza-Consejo Superior de Investigaciones Científicas, Pedro Cerbuna 12, 50009-Zaragoza, Spain

[‡]King Fahd University of Petroleum and Minerals, KFUPM Visiting Professor, Dhahran 31261, Saudi Arabia

Supporting Information

ABSTRACT: The [8,8,8-(H)(PPh$_3$)$_2$-9-(Py)-*nido*-8,7-RhSB$_9$H$_9$] (**2**)/[1,1-(PPh$_3$)$_2$-3-(Py)-*closo*-1,2-RhSB$_9$H$_8$] (**3**) pair catalyzes the hydrogenation of olefins through *nido*-to-*closo* transformations. Substitution of the phosphine ligands can lead to an improvement of the catalytic activity of this system. Therefore, the substitutional chemistry of **2** with PMePh$_2$, PMe$_2$Ph, and PMe$_3$ has been studied, leading to the formation of [8,8,8-(H)(PPh$_3$)(PR$_3$)-9-(Py)-*nido*-8,7-RhSB$_9$H$_9$], where R$_3$ = Me$_2$Ph (**5**) or Me$_3$ (**6**), and [8,8,8-(H)(PR$_3$)$_2$-9-(Py)-*nido*-8,7-RhSB$_9$H$_9$], where R$_3$ = MePh$_2$ (**4**) or Me$_2$Ph (**7**). Kinetic studies on the reaction of PMe$_2$Ph with **2** indicate that the substitutions follow a dissociative mechanism. The thermal dehydrogenation of **5**−**7** affords the corresponding *closo*-derivatives [1,1-(L)(PPh$_3$)-3-(Py)-*closo*-1,2-RhSB$_9$H$_8$], where L = PMe$_2$Ph (**9**) or PMe$_3$ (**10**), and [1,1-(L)$_2$-3-(Py)-*closo*-1,2-RhSB$_9$H$_8$], where L = PMe$_2$Ph (**11**) or PMe$_3$ (**12**). The substitution of PPh$_3$ by the more basic, less bulky phosphines facilitates hydrogen loss and consequent *nido*-to-*closo* transformations. The reaction of **5** and **6** with C$_2$H$_4$ promotes a *nido*-to-*closo* cluster change and the consequent formation of **10** and **11** together with small amounts of C$_2$H$_4$-ligated [1,1-(η^2-C$_2$H$_4$)(L)-3-(Py)-*closo*-1,2-RhSB$_9$H$_8$], where L = PPh$_3$ (**13**) or PMe$_3$ (**15**), characterized *in situ* by ^{1}H NMR spectroscopy. In the reactions with ethylene, ethane is detected *in situ*, indicating that the olefin is hydrogenated. The reactions of **5** and **6** with CO afford the CO-ligated [1,1-(CO)(L)-3-(Py)-*closo*-1,2-RhSB$_9$H$_8$], where L = PMe$_2$Ph (**16**) or PMe$_3$ (**17**). The reactivity of the new PR$_3$-ligated *nido*-clusters versus H$_2$, C$_2$H$_4$, and CO is not improved with the phosphines studied in this work; however, the changes found in the chemical beahavior of this system are dramatic, confirming the tailorability of these 11-vertex rhodathiaboranes and the potential optimization of their catalytic activity by the judicious choice of the *exo*-polyhedral ligands.

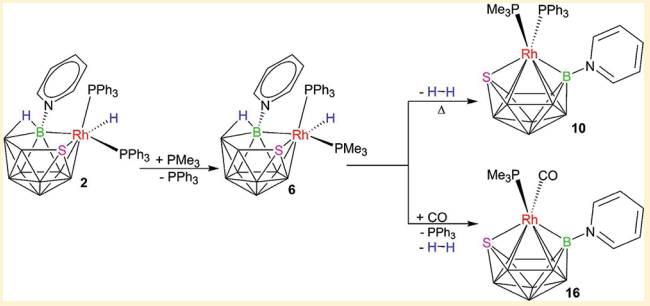

INTRODUCTION

In recent years, we have developed the chemistry of pyridine-ligated 11-vertex rhodathiaboranes that are synthesized from [8,8-(PPh$_3$)$_2$-*nido*-8,7-RhSB$_9$H$_{10}$] (**1**).[1] In particular, the system formed by [8,8,8-(H)(PPh$_3$)$_2$-9-(Py)-*nido*-8,7-RhSB$_9$H$_9$] (**2**) and [1,1-(PPh$_3$)$_2$-3-(Py)-*closo*-1,2-RhSB$_9$H$_8$] (**3**) has been found to give rise to an interesting reaction chemistry that embraces (i) *nido*-to-*closo* deshydrogenation, (ii) dihydrogen promoted *closo*-to-*nido* transformations, (iii) oxidative addition of sp C−H bonds, and (iv) catalysis of hydrogenation and isomerization of olefins (Scheme 1).[2]

These 11-vertex clusters are easily prepared, versatile, and stable, and, in view of the reactivity above-commented, they are compounds with potential as homogeneous catalyst precursors. Therefore, in an attempt to modify the reactivity of these clusters, we have already carried out substitution of the *exo*-polyhedral PPh$_3$ ligands in **1** with the more basic (less bulky) monodentate phosphines PMe$_3$, PMe$_2$Ph, and PPh$_2$Me.[3] The results of this work have provided new rhodathiaboranes [8,8-(PPh$_3$)(PR$_3$)-*nido*-8,7-RhSB$_9$H$_{10}$], where R$_3$ = Me$_3$ and Me$_2$Ph, and [8,8-(PMePh$_2$)$_2$-*nido*-8,7-RhSB$_9$H$_{10}$], which (*a priori*) were convenient starting materials for the synthesis of new hydridorhodathiaboranes derived from **2**; however, as these compounds are obtained as mixtures with the corresponding tris-PR$_3$-ligated species, [8,8,8-(PR$_3$)$_3$-*nido*-8,7-RhSB$_9$H$_{10}$], separatory work was necessary for the isolation of the clusters in moderate to low yields. In view of these results,[3] and as a continuation of our systematic tailoring of the 11-vertex rhodathiaborane system **2**/**3**, we decided to study the substitutional chemistry of **2**.

Here we describe the reactivity of compound **2** with PMePh$_2$, PMe$_2$Ph, and PMe$_3$, the subsequent preparation of new 11-vertex hydrido-Rh *nido*-clusters, and the study of their

Received: October 1, 2011
Published: March 27, 2012

   dx.doi.org/10.1021/om2009205 | *Organometallics* 2012, 31, 2986−2995

Scheme 1. Formation of 2 and Ethylene Dihydrogen Mediated *nido* → *closo* → *nido* Conversion

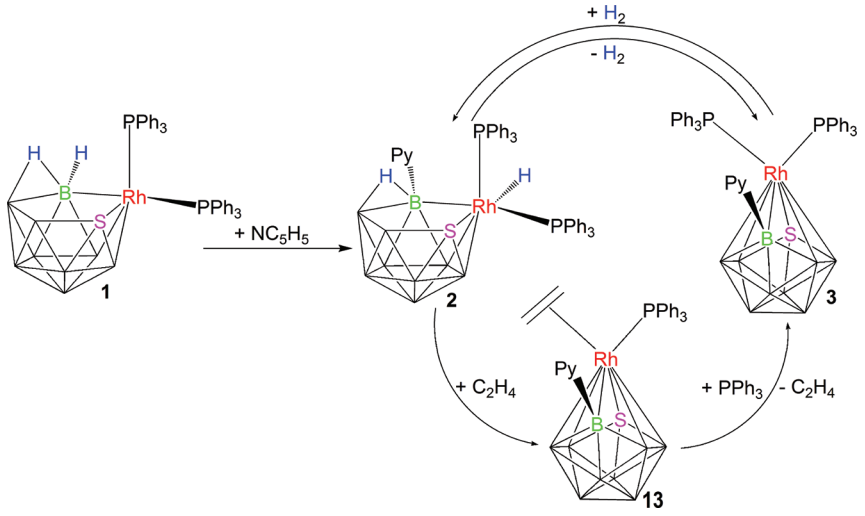

Scheme 2

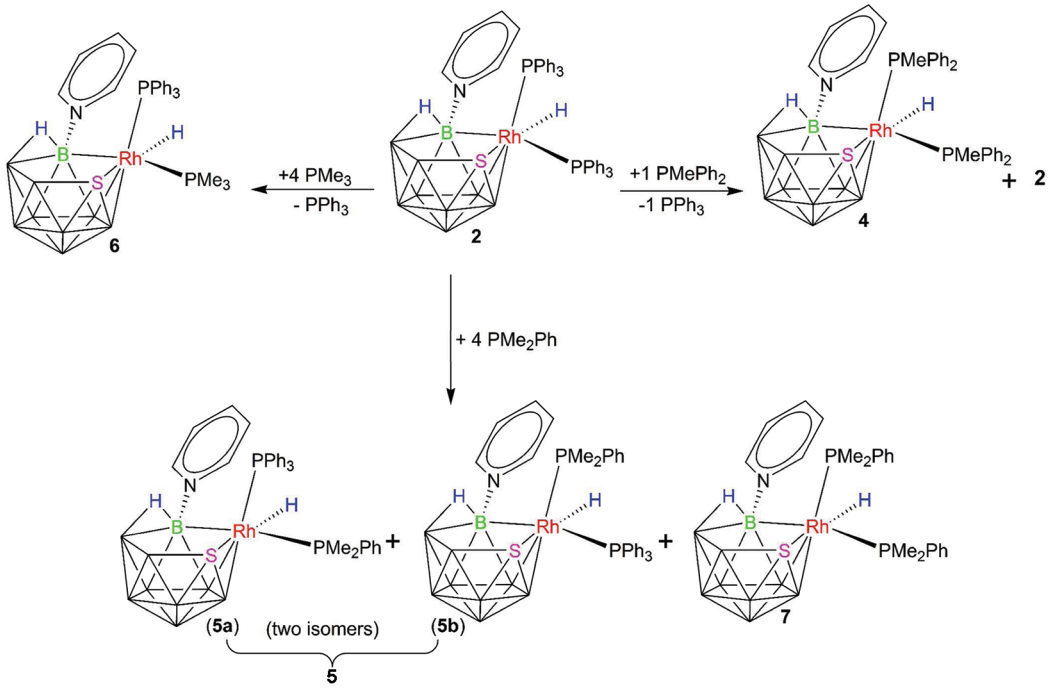

reactivity with small molecules such as CO, C_2H_4, and H_2, discussing trends and differences within the new series of PR_3-ligated clusters and with the previously reported PPh_3-ligated counterparts **2** and **3**.

RESULTS AND DISCUSSION

Reactions of [8,8,8-(H)(PPh$_3$)$_2$-9-(Py)-*nido*-8,7-RhSB$_9$H$_9$] (2) with PR$_3$. Treatment of the bis-PPh_3-ligated compound **2** with one equivalent of phosphine PR_3 affords [8,8,8-(H)(PPh_3)(PR_3)-9-(Py)-*nido*-8,7-$RhSB_9H_9$], where R_3 = Me_2Ph (**5**) or Me_3 (**6**). A 1 to 4 molar ratio of **2** versus PMe_3 yields also the monosubstitued hydrido cluster **6**, whereas the reaction of **2** with four equivalents of PMe_2Ph affords the mixture, **5**, which contains two monosubstituted isomers (*vide infra*) **5a** and **5b** and the disubstitutued [8,8,8-(H)(PMe_2Ph)$_2$-9-(Py)-*nido*-8,7-$RhSB_9H_9$] (**7**) (Scheme 2). In interesting contrast, the reaction of **2** with $PMePh_2$ in a 1:1 molar ratio gives mixtures that contain the new disubstituted species [8,8,8-(H)($PMePh_2$)$_2$-9-(Py)-*nido*-8,7-$RhSB_9H_9$] (**4**) and the starting **2** (Scheme 2). The new 11-vertex hydridorhodathiaboranes **4**–**7** have been characterized by multinuclear NMR spectroscopy and mass spectrometry. In addition, a solid-state X-ray diffraction analysis confirmed the molecular structure of **4** (Figure 1).

These rhodathiaboranes have an 11-vertex {$RhSB_9$} core geometry, formally derived from an icosahedron by the removal of a vertex, which resembles the structures of the pyridine-ligated counterpart **2**[2a] and the $PMePh_2$-B(9)-substituted [8,8,8-(H)($PMePh_2$)$_2$-9-($PMePh_2$)-*nido*-8,7-$RhSB_9H_9$] (**8**).[3] The framework structures correspond exactly to what one expects for a 13-skeletal electron pair (sep) cluster with 11 vertices.[4] This contrasts with the formal unsaturation found in the parent compound, **1**,[1] which has only 12 sep, but a *nido* structure. The discrepancy between the number of sep and the structure is an interesting feature of 11-vertex heteroborane

dx.doi.org/10.1021/om2009205 | *Organometallics* 2012, 31, 2986–2995

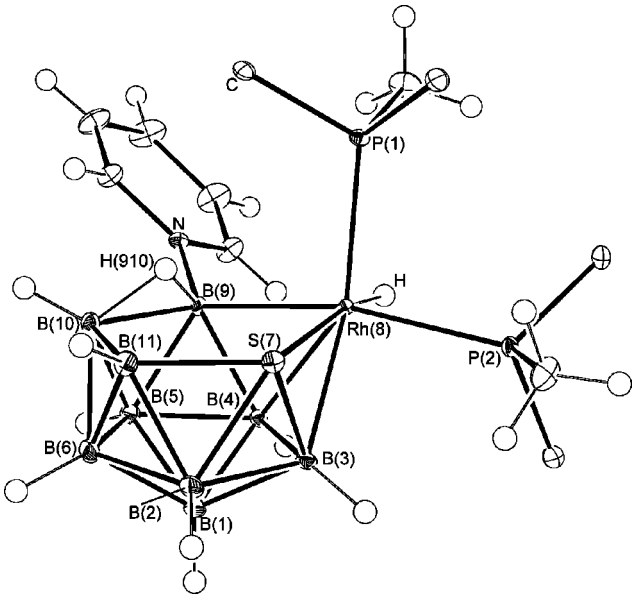

Figure 1. Molecular structure of compound **4**. Only the *ipso*-carbon atoms on the phenyl groups are included to aid clarity. Ellipsoids are shown at 50% probability level. Selected interatomic distances [Å] and angles [deg]: Rh(8)−S(7) 2.4270(5), Rh(8)−P(1) 2.3091(6), Rh(8)−P(2) 2.3224(6), Rh(8)-H 1.53(4), Rh(8)−B(3) 2.230(2), Rh(8)−B(4) 2.209(2), Rh(8)−B(9) 2.214(2), B(9)-N 1.556(3); P(1)−Rh(8)−P(2) 98.10(2), P(1)−Rh(8)−S(7) 105.08(2), P(2)−Rh(8)−S(7) 97.82(2), P(1)−Rh(8)−B(9) 95.66(6), P(2)−Rh(8)−B(9) 163.22(6), P(1)−Rh(8)−B(3) 157.35(7), P(1)−Rh(8)−B(4) 141.17(6), P(2)−Rh(8)−B(3) 87.61(6), P(2)−Rh(8)−B(4) 116.59(6), S(7)−Rh(8)−H 168.2(14).

frameworks that incorporate $\{Rh(L)_2\}$ or $\{Pt(L)_2\}$ (L = phosphine ligands) fragments,[5] making them intrinsically Lewis acidic and, therefore, potentially labile. The Rh(8)−S(7) distance of 2.4270(5) Å in **4** is close to the values found for the previously reported analogue **2** (Schemes 1 and 2) and **8** (Chart 1, I),[2a,3] where the hydride ligand is also *trans* to the

Chart 1

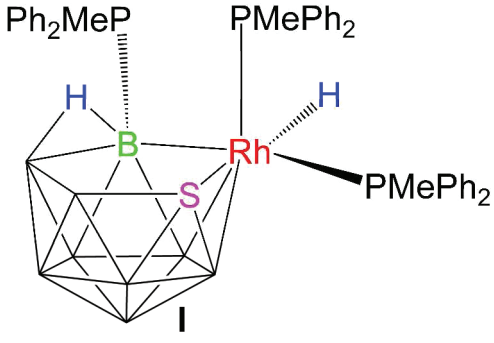

I

S(7) vertex (Table 1). In contrast, the Rh(8)−S(7) distance is ca. 0.05 Å shorter in tris-PR_3-ligated *nido*-rhodathiaboranes that bear a phosphine ligand *trans* to the sulfur atom,[3] confirming the high structural *trans* influence of the hydride ligand (Table 1). It is interesting to note that Rh−P distances in the $PMePh_2$-ligated cluster **4** are ca. 0.03 Å shorter than the corresponding values in the PPh_3 analogue **2**, reflecting the higher σ-donor capabilities of $PMePh_2$ and its smaller steric hindrance. In **2**, **4**, and **8**, the longest Rh−P distance corresponds to the phosphine ligand *trans* to the substituted

Table 1. *trans*-Effect of the Hydride Ligand in Some 11-Vertex *nido*-Rhodathiaboranes

compound	Rh(8)−S(7) (Å)	ref
$[(PPh_3)_2RhSB_9H_{10}]$ (**1**)[a]	2.3769(6)	1
$[(PMePh_2)_3RhSB_9H_{10}]$[a]	2.3757(8)	6
$[(PMe_3)_3RhSB_9H_{10}]$[a]	2.3736(7)	3
$[(H)(PPh_3)_2RhSB_9H_9(Py)]$ (**2**)[b]	2.431(2)	2b
$[(H)(PMePh_2)_2RhSB_9H_9(Py)]$ (**4**)[b]	2.4271(5)	this work
$[(H)(PMePh_2)_2RhSB_9H_9(PMePh_2)]$ (**8**)[b]	2.4172(5)	3

[a]Non-hydride-containing cluster. [b]Hydride-containing cluster.

9-position of the cluster, and the difference between the two Rh−P distances within each cluster is ca. 0.013(2) Å.

The structure of **4** is consistent with its spectroscopic data and those of the analogues, **2**, **5** (mixture of isomers), **6**, and **7**. In this type of compound, the ^{11}B NMR resonances are found in the interval between $\delta(^{11}B)$ +12.0 and −28.0 ppm. The pattern does not change significantly through the series, with the boron-11 resonance at the lowest field assigned to the pyridine-ligated boron atom at the 9-postion.

The Rh−H hydride and B−H−B bridging hydrogen resonances are quite informative, serving as diagnostic for the formation of these clusters. The hydride signal appears close to $\delta(^1H)$ −12.5 ppm in the series: an apparent quartet for the bis-PPh_3- and bis-$PMePh_2$-ligated clusters, **2** and **4**, and a doublet of doublets of doublets for the monosubstituted analogue **6**. In contrast, the PMe_2Ph-monosubstituted counterpart **5** exhibits two hydride resonances in a 1:0.6 ratio, indicating the presence of two isomers (**5a** and **5b**, Scheme 2).

Scheme 3 depicts the shift of the hydride ^1H resonance found in **2** and **4**−**7**. Monosubstitution with PMe_2Ph and PMe_3 at the position *trans* to the B(9) vertex results in a shielding of the signal, the shift being larger for the more basic phosphine, PMe_3. It appears that substitution at the position *trans* to the B(3)−B(4) edge results in a smaller high-field shift of the hydride resonance (**5b** vs **5a**).

An interesting characteristic that these Py-ligated hydrido-rhodathiaboranes share is the temperature-dependent behavior of their $^{31}P\{^1H\}$ NMR spectra (see Figures 2, S1, and S2). Thus, one of the phosphorus resonances is significantly broader than the other at room temperature, and it sharpens as the temperature is decreased. First discovered for compound **2** (Figure S2), it was thought that this behavior is consistent with a dissociation of the PPh_3 ligand *trans* to the B(9) vertex.[2b] However, this conclusion should be put into question since the broadening could be due to $^{31}P-^{11}B$ couplings, which at lower temperatures are reduced due to the thermal decoupling of the quadrupolar ^{11}B (I = 3/2) nucleus.[7]

The $^{31}P\{^1H\}$ spectra of compounds **4** and **6** are assigned on the basis of the commented relative broadening of the peaks and the well-differentiated low-field chemical shift of the PPh_3 ligand with respect to $PPhMe_2$ and PMe_3. The assignments for the isomers **5a** and **5b** and the bis-PPh_2Me-ligated cluster **7** were made by analysis of a series of ^1H, $^1H\{^{31}P\}$, $^{31}P\{^1H\}$, and $^1H-^{31}P$ HSQC spectra (see Figures S8 to S14).

Substitution Reactions: Mechanistic Considerations. In order to obtain some mechanistic insights into the substitutional chemistry of **2** with monodentate phosphines, small-scale reactions were studied at low temperatures by NMR spectroscopy. Upon the addition of one equivalent of PMe_3 to a CD_2Cl_2 solution of **2** at 188 K, the $^{31}P\{^1H\}$ spectrum exhibits the signals of compound **2**, free PPh_3, and PMe_3 (Figure 2).

dx.doi.org/10.1021/om2009205 | *Organometallics* 2012, 31, 2986−2995

Scheme 3. Illustration of the ^{1}H Chemical Shift of the Rh−H Hydride Ligand

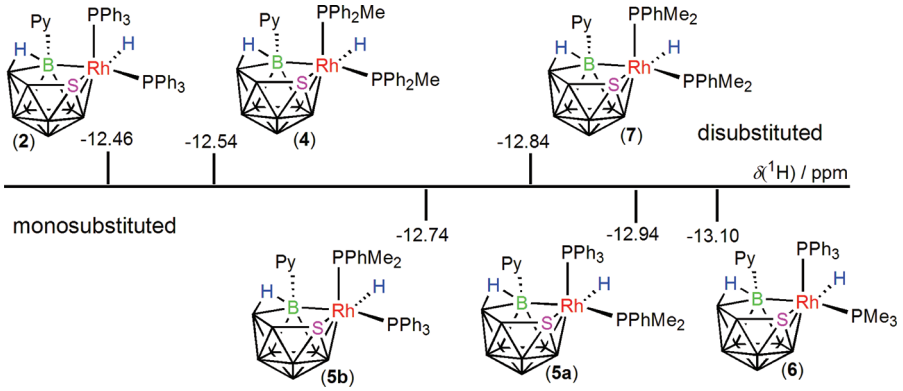

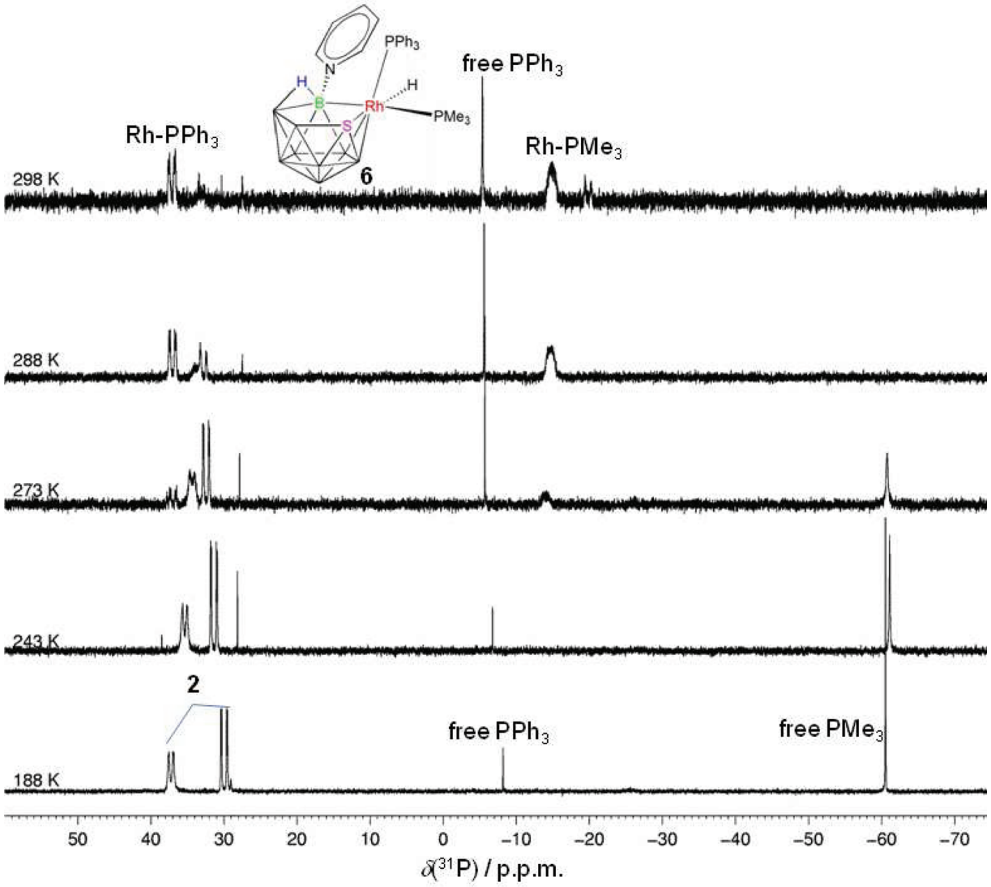

Figure 2. Variable-temperature $^{31}P\{^{1}H\}$ NMR spectra of **2** upon addition of one equivalent of PMe_3 at low temperature (bottom spectrum).

The resonances of the substitution product **6** are not well detected in the $^{31}P\{^{1}H\}$ spectra until the temperature reaches 273 K. At room temperature, the reaction is completed [Figure 2: the broadness of the resonance close to $\delta(^{31}P)$ −15.0 ppm arises most probably from $^{2}J(^{31}P-^{11}B)$ coupling as commented above]. The proton NMR spectrum reflects these results, showing the disappearance of the starting material **2** and the consequent formation of its substitution product **6** (Figure S3). There is also a weak Rh−H hydride signal at −12.70 ppm, which may correspond to a minor {Rh(H)-$(PMe_3)(PPh_3)$}-to{$SB_9H_9(Py)$} isomer. In any event, these data reveal that the reaction of **2** with PMe_3 affords the monosubstituted product **6** with good regioselectivity: the substitution takes place at the *exo*-polyhedral position that is *trans* to the B(9) vertex. Following the same procedure, the treatment of **2** with one equivalent of PMe_2Ph at low temperatures does not afford significant amounts of substitution products until the temperature reaches 273 K (see Figures S4 and S5). At room temperature, there is no free PMe_2Ph left and there are two sets of major signals in the $^{31}P\{^{1}H\}$ NMR spectrum. As commented above, the spectrum is consistent with the presence of two {Rh(H)$(PPh_3)(PMe_2Ph)$ }-to-{$SB_9H_9(Py)$} isomers: the signals at the lowest field are assigned to the PPh_3 ligands, whereas the peaks at around $\delta(^{31}P)$ −5 ppm correspond to the PMe_2Ph groups. In the same conditions, the reaction of **2** with one equivalent of $PMePh_2$ also starts to take place at significant rates above 273 K (see Figures S6 and S7), but in contrast, there is formation of the $PMePh_2$-disubstituted cluster, **4**.

dx.doi.org/10.1021/om2009205 | *Organometallics* 2012, 31, 2986−2995

These results indicate clearly that the reactions of the monodentate phosphines, $PMePh_2$, PMe_2Ph, and PMe_3, with **2** occur at lower rates than with the previously studied rhodathiaborane, **1**.[3] Variable-temperature experiments suggested that the most plausible mechanism for the substitution of the phosphine ligands in the parent compound **1** (Scheme 1) is associative, implying the binding of a third phosphine at the rhodium center.[3] For the herein described reactions of **2** with monodentate phosphines, however, it is not clear if, as discussed above, the broadening of one of the two ^{31}P resonances in this new series of hydridorhodathiaboranes, **4**–**7**, is due to $^{31}P-^{11}B$ coupling or to dissociative processes (or both).

In compound **6**, DFT calculations have confirmed the assignment of the broad ^{31}P signal at the highest field as the PMe_3 ligand *trans* to the pyridine-substituted B(9) vertex (Table S10); in addition, previous DFT studies revealed that elongation of the $Rh-PH_3$ bond *trans* to the B(9)–Py vertex in the model [8,8,8-(H)$(PH_3)_2$-9-(Py)-*nido*-8,7-$RhSB_9H_9$] results in a smaller energy increase of the cluster compared with the elongation of the $Rh-PH_3$ bond *trans* to the B(3)–B(4) edge.[2b] Thus, these theoretical results suggest that dissociation of the PR_3 ligand *trans* to the {B(9)–Py} vertex in **2** and **4**–**7** may play an important role in the reactivity of these clusters.

Kinetic Studies. The following kinetic studies try to shed more light on the reaction mechanism. The reaction between **2** and PMe_2Ph was studied by ^1H NMR spectroscopy, monitoring the decrease of the hydride integral resonance versus time. The concentration of PMe_2Ph was kept in excess to hold pseudo-first-order conditions. The value of k_{obs}, summarized in Table 2, is independent of the concentration of PMe_2Ph, suggesting that the substitution of one PPh_3 ligand in **2** takes place in a dissociative process. The activation parameters obtained from the Eyring plot (Figure S15), $\Delta H^{\ddagger} = 33 \pm 3$ kcal mol^{-1} and $\Delta S^{\ddagger} = 45 \pm 9$ eu, are consistent with dissociation of PPh_3 as the most plausible mechanism for this reaction. Therefore, although the commented-above temperature-dependent broadening in the $^{31}P\{^1H\}$ spectra of **2**–**7** may arise mainly from the effects of "thermal decoupling" on the boron nuclei, dissociation of the phosphine ligand *trans* to B(9), as previously suggested by us,[2b] appears to direct the reactivity of these clusters.

Table 2. Rate Constants for PPh_3 Substitution in Compound 2[a]

T (K)	[PMe_2Ph] (equivalents)	$10^2 k_{obs}$ (min^{-1})[b]
273	5	1.4
273	20	1.4
263	10	0.13
268	10	0.27
273	10	1.4
279	10	2.5
283	10	14.3

[a][**2**] = 0.02 M in CD_2Cl_2. [b]Values obtained from three different measurements.

Reactivity Studies. The modification of the *exo*-polyhedral ligands in the 11-vertex rhodathiaboranes **2** and **3** is a reasonable approach for the fine-tuning of the reactivity of this system. The adequate combination of *exo*-polyhedral ligands bound either to the rhodium atom or to the B(9) vertex can (*a priori*) result in an improvement of the catalytic activity of this kind of cluster. Therefore, we carried out a systematic study of the reactivity of the new PR_3-ligated clusters, **4**–**7**, having the PPh_3-ligated clusters **2** and **3** as reference.

Dehydrogenation. The hydridorhodathiaboranes **2** and **5**–**7** are stable in solution at room temperature; however, heating at reflux temperature in dichloromethane results in the loss of dihydrogen and the concomitant *nido*-to-*closo* transformation of the clusters (Scheme 4). In contrast, the $PMePh_2$-ligated counterpart, **4**, does not undergo dehydrogenation. Quantitative studies on the dehydrogenation reactions were carried out by ^1H NMR spectroscopy at 50 °C in CD_2Cl_2 (Tables S4–S6). The results were adjusted to first-order kinetics, yielding the reaction rates and half-life constants listed in Table 3.

Table 3. Rate Constants and Half-Lives for the Dehydrogenation Reactions of 2, 5a, 5b, 6, and 7 in CD_2Cl_2 at 50 °C

compound	$k \times 10^4$ min^{-1}	$t_{1/2}$ (h)
2	26 ± 1.4	4.4
5a	41 ± 0.5	2.8
5b	25 ± 0.4	4.6
6	45 ± 1.6	2.6
7	83 ± 1.5	1.4

These data show that the fastest rate of dehydrogenation corresponds to the bis-PMe_2Ph-ligated **7**: roughly three times as fast as the parent cluster **2** and the isomers **5b**. Next in the series, we find the isomer **5a** and the PMe_3-monosubstituted derivative **6**, which exhibit a rate of dehydrogenation approximately two times faster than **2** (and **5b**). This trend indicates that the substitution of PPh_3 with more basic and less bulky phophine lingads facilitates the dehydrogenation of the clusters and the consequent *nido*-to-*closo* transformation. In addition, the different rate between the isomers **5a** and **5b** suggests that a *trans* arrangement of PR_3, where $R_3 = Me_2Ph$ (**5a** and **5b**) and Me_3 (**6**), to the B(9) vertex results in an increase of the dehydrogenation rate. It is somewhat surprising,

Scheme 4

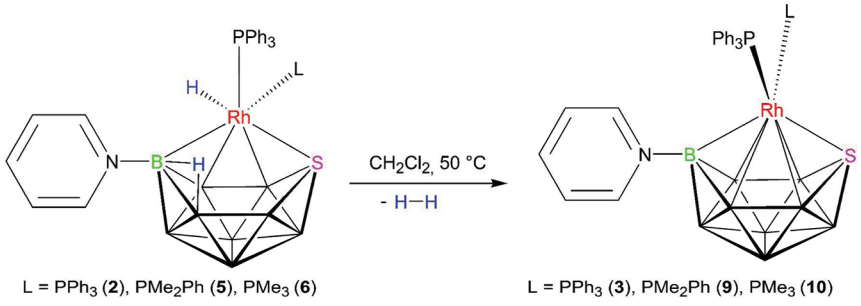

dx.doi.org/10.1021/om2009205 | *Organometallics* 2012, 31, 2986–2995

however, that in the same conditions hydrogen loss is completely hindered for the $PMePh_2$-ligated compound **4**.

The thermal treatment of **5**, **6**, and **7** is a convenient route to the synthesis of the mixed-ligated *closo*-derivatives [1,1-(L)(PPh_3)-3-(Py)-*closo*-1,2-$RhSB_9H_8$], where L = PMe_2Ph (**9**) or PMe_3 (**10**), and the bis-PR_3-ligated analogues [1,1-(PR_3)$_2$-3-(Py)-*closo*-1,2-$RhSB_9H_8$], where L = PMe_2Ph (**11**) or PMe_3 (**12**). These compounds have been fully characterized by multinuclear NMR and mass spectrometry. X-ray diffraction analysis has confirmed the molecular structures of **10** and **11** (Figures 3 and Figure S16, respectively).

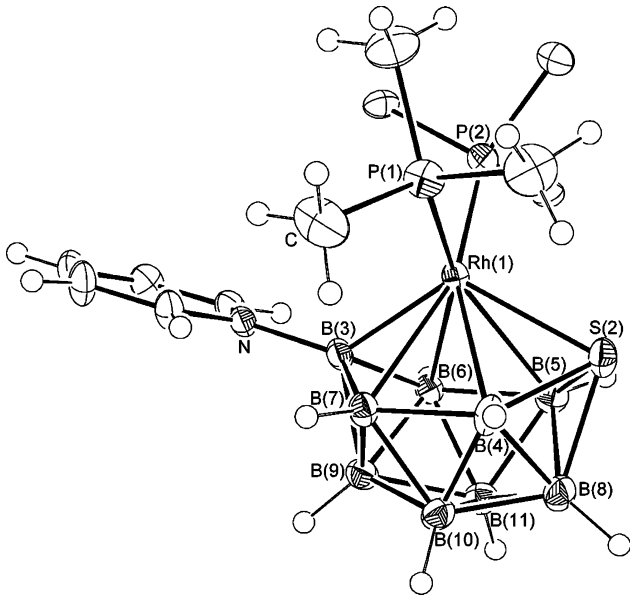

Figure 3. Molecular structure of **10**. Only the *ipso*-carbon atoms on the phenyl rings of the PPh_3 ligand are included to aid clarity. Ellipsoids are shown at 50% probability level. Selected interatomic distances (Å) and angles (deg): Rh(1)−S(2) 2.3841(9), Rh(1)−P(1) 2.2889(10), Rh(1)−P(2) 2.2710(9), Rh(1)−B(3) 2.087(4), Rh(1)−B(4) 2.401(4), Rh(1)−B(5) 2.471(4), Rh(1)−B(6), 2.380(4), Rh(1)−B(7) 2.354(4); P(1)−Rh(1)−P(2) 96.68(4).

The molecular structures of **10** and **11** are based on the canonical structure of an octadecahedron that may be rationalized by simple application of the Wade/Mingos approach.[4] The rhodium atom occupies the apical cluster position connected to six atoms in the {SB_9} fragment with two *exo*-polyhedral metal coordination sites occupied by the PPh_3 and PR_3 ligands. Compounds **9**−**12** are isoelectronic with **3** and the organometallic derivatives [1,1-(η^2-L)(PPh_3)-3-(Py)-*closo*-1,2-$RhSB_9H_8$], where L = η^2-C_2H_4 (**13**, Scheme 1 above) or η^2-$C_2(CO_2Me)_2$,[2c] as well as other rhodathiaboranes that have different *exo*-polyhedral ligands on the rhodium center and the B(3) vertex.[2c,8] Not surprisingly, the longest Rh−P distance [2.3278(13) Å] corresponds to **3**, which bears two bulky PPh_3 ligands; however, it is interesting to notice that in **10** the P−Rh distance of the PMe_3 ligand [2.2889(10) Å] is longer than that of PPh_3 [2.2710(9) Å], suggesting that the steric effects of PPh_3 dominate the better σ-donor capabilities of PMe_3.

Reactions with H_2(g). The *closo*-rhodathiaborane **3** reacts with dihydrogen to give the *nido*-cluster **2**.[2a] This is a significant reaction that implies the heterolytic splitting of H_2 on the *closo*-cluster and completes a stoichiometric cycle of dehydrogenation/hydrogenation that represents the essence of the catalytic activity of the system (see Scheme 1 above).[2b] Therefore, one of the objectives of this work was to change the phosphine ligands to optimize the activation of dihydrogen by 11-vertex *closo*-rhodathiaboranes and subsequently the transfer of the two hydrogen atoms to unsaturated organic molecules. However, in the same conditions as **3**, the 11-vertex *closo*-rhodathiaboranes **9**−**12** do not react with dihydrogen. Thus, although the loss of H_2 is facilitated by the presence of the more basic and less bulky PMe_2Ph and PMe_3 ligands in **5**−**7**, the reverse reaction with H_2 (to regenerate these *nido*-hydrido clusters) is hindered. In other words, the energy barrier for the dehydrogenation of the *nido*-clusters is lower than for the PPh_3-ligated compound **2**, whereas the activation energy of the reaction of the 11-vertex *closo*-rhodathiaboranes **9**−**12** with H_2 appears to be higher than for **3**, precluding the H_2 addition to the *closo*-clusters. In this context, once more, it is noteworthy that **4** does not undergo hydrogen loss in the same conditions as **2** and **5**−**7**, indicating that for the $PMePh_2$-ligated counterpart the activation energy barrier toward the formation of the hypothetical *closo*-cluster, [1,1-($PMePh_2$)$_2$-3-(Py)-*closo*-1,2-$RhSB_9H_8$], by loss of H_2 is significantly higher. In any event, it is evident that the nature of the phosphine ligands plays a crucial role in tuning the reactivity of the *closo*-cluters toward the activation of dihydrogen; therefore, the right choice of ligands should improve the reactivity of the system toward small molecules.

Reactions with CO and C_2H_4. Both reagents CO and C_2H_4 react with **2** to give CO- and C_2H_4-ligated *closo*-rhodathiaboranes [1,1-(L)(PPh_3)-3-(Py)-*closo*-1,2-$RhSB_9H_8$], where L = C_2H_4 (**13**, Scheme 1 above) or CO (**14**, Chart 2, II);[2a,b] in the reaction with ethylene, there is also formation of ethane (detected *in situ* by ^{1}H NMR spectroscopy), demonstrating that the alkene is hydrogenated. In the current study, it has been found that the reaction of **5** (mixture of isomers) and **6** with ethylene promotes the *nido*-to-*closo* transformation, yielding **10** and **11**, respectively, at room temperature, also formed thermally in longer reaction times as discussed above. Under a higher pressure of ethylene (see Experimental Section), the reaction of **6** has been found to afford, in addition to the major component **10**, small amounts of the ethylene-ligated rhodathiaborane, **13**, and the PMe_3-ligated counterpart, [1,1-(η^2-C_2H_4)(PMe_3)-3-(Py)-*closo*-1,2-$RhSB_9H_8$] (**15**). This new compound has been characterized *in situ* by NMR spectroscopy, and the chemical nonrigidity of the Rh−C_2H_4 linkage studied by variable-temperature ^{1}H NMR experiments (Figure S17). The activation energy of this rotational fluxional process is 4 kJ/mol higher for **15** than for **13**, suggesting a stronger Rh−(η^2-C_2H_4) bond as the result of an increase in the

Chart 2

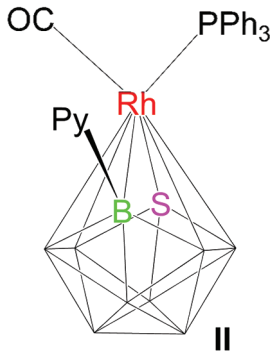

II

dx.doi.org/10.1021/om2009205 | *Organometallics* 2012, 31, 2986−2995

Scheme 5

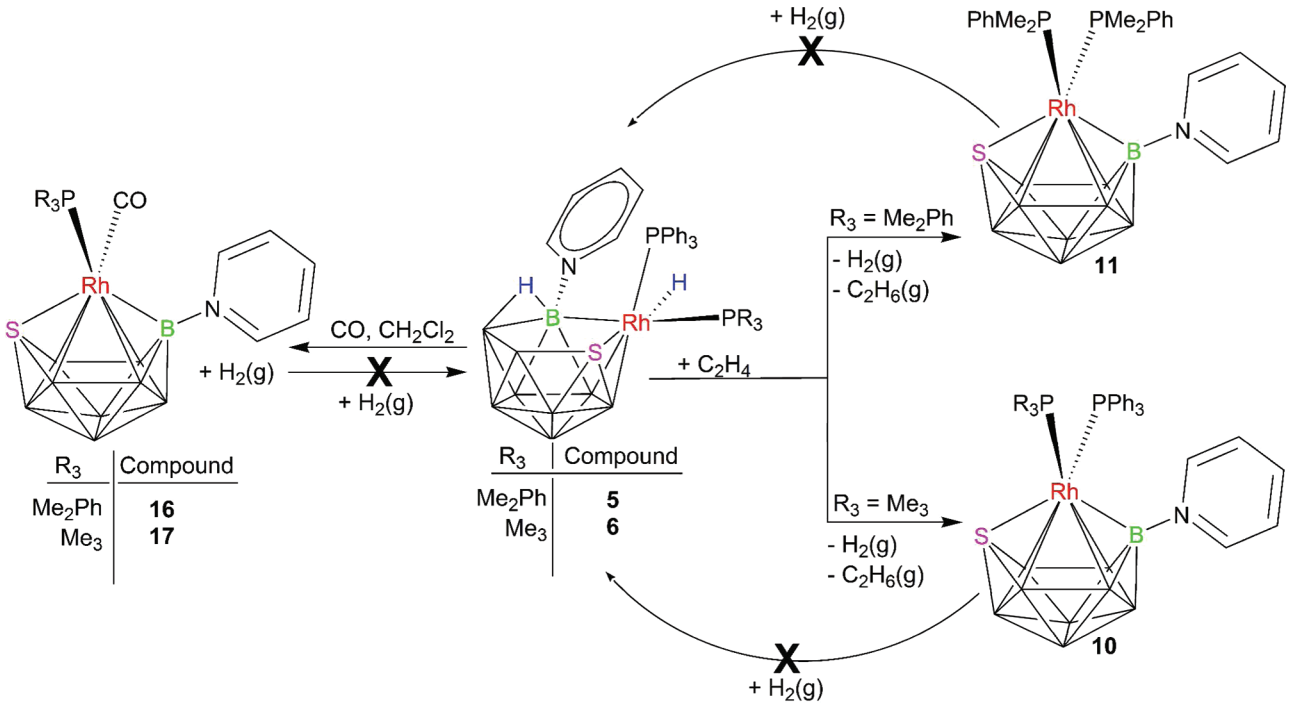

π-back-donation from the metal center to the olefin ligand in the former compound, which is expected from the presence of the better σ-donor ligand, PMe_3 in **15**. In the same conditions, in contrast, the mixture of isomers **5** leads to only **13** in small amounts. Both reactions afford ethane (**10**-to- and **11**-to-C_2H_6 ratio 1:0.2), indicating that although the major reaction appears to be H_2 loss, the transfer of the two hydrogen atoms to the C═C bond of the olefin also occurs for the new PR_3-ligated hydrido-ligated clusters (Scheme 5).

With carbon monoxide, the mixture of isomers **5** reacts to give the CO-ligated *closo*-cluster **14** (Chart 2, II) and the new derivative [1,1-(CO)(PMe_2Ph)-3-(Py)-*closo*-1,2-$RhSB_9H_8$] (**16**) in a 1:4 ratio. Similarly, compound **6** reacts to give a mixture of **14** and [1,1-(CO)(PMe_3)-3-(Py)-*closo*-1,2-$RhSB_9H_8$] (**17**), this time in a 1:5 ratio. Therefore, carbon monoxide substitutes one phosphine ligand in the hydridorhodathiaboranes, causing the *nido*-to-*closo* transformation of the cluster by hydrogen loss. The PPh_3 ligand is preferably substituted by the entering CO molecule, reflecting the fact that PMe_2Ph in **5** and PMe_3 in **6** are worse leaving groups than PPh_3.

CONCLUSIONS

The parent hydrido-Rh cluster **2** reacts readily with monodentate phosphines, affording new 11-vertex derivatives with compositions and configurations that depend on the entering phosphine. Thus the treatment of **2** with $PMePh_2$ forms exclusively the bis-substituted cluster **4**. In contrast, the less bulky and more basic phosphines PMe_3 and PMe_2Ph afford monosubstituted species **5** (mixture of isomers) and **6**; with PMe_2Ph, it is also possible to prepare the bis-substituted derivative **7**. Kinetic studies demonstrate that the substitution of the PPh_3 ligand in **2** follows a dissociative mechanism that most likely involves the phosphine ligand *trans* to the B(9) position. These results support previous conclusions dealing with the reactivity of **2** with olefins in which dissociative mechanisms were invoked.[2a,b]

The new 11-vertex *nido*-hydridorhodathiaboranes, **5**−**7**, undergo faster thermal dehydrogenation than the parent compound **2** to give the corresponding *closo*-clusters, **9**−**11**, which do not react with H_2 in the same reaction conditions used for the bis-PPh_3-ligated derivative **3**. Therefore, the dehydrogenation/hydrogenation cycle found for the bis-PPh_3-ligated **2**/**3** pair is not completed (in the conditions of pressure and temperature studied) with the new rhodathiaboranes reported in this work. Ethylene promotes hydrogen loss and consequent *nido*-to-*closo* transformation, but compared with **2**, the new species **5** and **6** do not exhibit an enhanced reactivity with the olefin; perhaps reflecting the fact that the dissociation of the Rh−PMe_2Ph and Rh−PMe_3 bonds in **5** and **6** is more difficult than the dissociation of Rh−PPh_3 in **2**. This fact together with the lack of reactivity of the new *closo*-clusters with dihydrogen, essential for subsequent hydrogenation of unsaturated organic molecules, indicates that the change of PPh_3 in **2** with the phosphines studied in this work would not lead to an improvement in the catalytic activity of the system. Likewise, the new CO-ligated *closo*-clusters **16** and **17** are inert in the presence of molecular hydrogen, matching this time the reactivity of the PPh_3-ligated counterpart **14**.

Although the objective of improving the reactivity of the **2**/**3** pair versus dihydrogen and olefins is not accomplished by substitution of PPh_3 with the studied phosphines, the treatment of **2** with PR_3, where R_3 = Me_3, Me_2Ph, and $MePh_2$, is a convenient synthetic route for the alteration of the *exo*-polyhedral ligand sphere, confirming the tailorability of this 11-vertex rhodathiaborane system. The lack of reactivity of the bis-$PMePh_2$-ligated cluster **4** is an interesting contrast, which suggests that other *exo*-polyhedral metal ligands may tune the clusters toward the opposite behavior: an enhancement of the catalytic activity with respect to **2**.

dx.doi.org/10.1021/om2009205 | *Organometallics* 2012, 31, 2986−2995

EXPERIMENTAL SECTION

General Procedures. Reactions were carried out under an argon atmosphere using standard Schlenk-line techniques. Solvents were obtained dried from a solvent purification system from Innovative Technology Inc. The commercially available phosphines PMe_3, PMe_2Ph, and $PMePh_2$ were used as received without further purification. The 11-vertex rhodathiaborane **2** was prepared according to the literature methods.[2a,b] Preparative thin-layer chromatography (TLC) was carried out using 1 mm layers of silca gel G (Fluka, type GF254) made from water slurries on glass plates of dimensions 20 × 20 cm and dried in air at 25 °C. Infrared spectra were recorded on a Perkin-Elmer Spectrum 100 spectrometer, using a Universal ATR sampling accessory. NMR spectra were recorded on Bruker Avance 300-MHz and AV 400-MHz spectrometers, using $^{31}P\{^1H\}$, ^1H-^{31}P HSQC, ^{11}B, $^{11}B\{^1H\}$, ^1H, $^1H\{^{11}B\}$, and $^1H\{^{11}B(selective)\}$ techniques. ^1H NMR chemical shifts were measured relative to partially deuterated solvent peaks but are reported in ppm relative to tetramethylsilane. ^{11}B chemical shifts are quoted relative to $[BF_3(OEt)_2)]$, and ^{31}P chemical shifts are quoted relative to 85% aqueous H_3PO_4. Mass spectrometric data were recorded on a MICROFLEX instrument operating in either positive or negative modes, using matrix-assisted laser desorption/ionization (MALDI). A nitrogen laser of 337 nm (photon energy of 3.68 eV) was used for the ionization processes, and the molecules under study were protected with a matrix of *trans*-2-[3-(4-*tert*-butylphenyl)-2-methyl-2-propenylidene]malononitrile.

X-ray Crystallography. Crystals of compounds **4**, **10**, and **11** suitable for X-ray diffraction analysis were grown by slow diffusion of hexane into a concentrated solution of each rhodathiaborane in dichloromethane. X-ray diffraction data were collected at low temperature (100(2) K) on the BM16 CRG beamline at the ESRF in the case of **4**, and for **10** and **11** using an automatic Bruker Kappa APEX DUO CCD area detector diffractometer equipped with graphite-monochromatic Mo Kα radiation (λ = 0.71073 Å) using narrow frames (0.3° in ω). In all cases, single crystals were mounted on micromount supports and were covered with a protective perfluoropolyether. In the case of **4**, data were measured in a single-axis HUBER diffractometer, equipped with an Oxford 600 Cryosystem open-flow nitrogen cryostat (100(1) K), using monochromatic silicon(111) synchrotron radiation (λ = 0.7382 Å). Intensities were integrated including Lorentz and polarization effects with the HKL2000 suite (**4**) or SAINT-Plus program[9] (**10** and **11**) and corrected for absorption using multiscan methods applied with the SORTAV (**4**) or SADABS (**10** and **11**) program.[10] The structures were solved using the SHELXS-86 program.[11] Refinements were carried out by full-matrix least-squares on F^2 with SHELXL-97,[12] including isotropic and subsequent anisotropic displacement parameters for all non-hydrogen atoms. All hydrogen atoms for compounds **4** and **10** were included from observed positions and refined isotropically. For **11**, most of the hydrogen atoms were observed, but some others were included in calculated positions and refined with a riding model. The programs ORTEP-3[13] and PLATON[14] were used to prepare the figures and the crystallographic data.

Crystal data for compound ***4****:* $C_{31}H_{41}B_9NP_2RhS{\cdot}2(CH_2Cl_2)$, M = 891.74; yellow block, 0.078 × 0.065 × 0.052 mm^3; monoclinic, $P2_1/n$; a = 10.1578(3) Å, b = 25.6316(2) Å, c = 16.3428(3) Å; β = 100.3430(10)°; Z = 4; V = 4185.88(15) Å^3; D_c = 1.415 g/cm^3; μ = 0.812 mm^{-1}, min. and max. correction factors 0.80 and 1.24; $2\theta_{max}$ = 56.24°; 42 060 reflections collected, 8895 unique [R_{int} = 0.0731]; number of data/restrains/parameters 8895/0/624; final GoF 1.058, R_1 = 0.0420 [8707 reflections, $I > 2\sigma(I)$], wR_2 = 0.112 for all data.

Crystal data for compound ***10****:* $C_{26}H_{37}B_9NP_2RhS \cdot CH_2Cl_2$, M = 742.69; red plate, 0.195 × 0.094 × 0.037 mm^3; triclinic, $P\bar{1}$; a = 10.8930(11) Å, b = 12.0718(12) Å, c = 14.3942(14) Å; α = 87.299(2)°, β = 69.5940(10)°, γ = 81.4180(10)°; Z = 2; V = 1754.1(3) Å^3; D_c = 1.406 g/cm^3; μ = 0.811 mm^{-1}, min. and max. transmission factors 0.798 and 0.943; $2\theta_{max}$ = 59.08°; 19 013 reflections collected, 8827 unique [R_{int} = 0.0474]; number of data/restrains/parameters 8827/0/544; final GoF 1.010, R_1 = 0.0481 [6398 reflections, $I > 2\sigma(I)$], wR_2 = 0.115 for all data.

Crystal data for compound ***11****:* $C_{21}H_{35}B_9NP_2RhS{\cdot}CH_2Cl_2$, M = 680.67; red prism, 0.203 × 0.149 × 0.117 mm^3; monoclinic, $P2_1/c$; a = 9.1278(13) Å, b = 24.263(4) Å, c = 14.915(2) Å; β = 103.397(2)°; Z = 4; V = 3213.2(8) Å^3; D_c = 1.407 g/cm^3; μ = 0.878 mm^{-1}, min. and max. transmission factors 0.798 and 0.902; $2\theta_{max}$ = 58.82°; 34 469 reflections collected, 8363 unique [R_{int} = 0.0270]; number of data/restrains/parameters 8363/4/470; final GoF 1.170, R_1 = 0.0591 [7700 reflections, $I > 2\sigma(I)$], wR_2 = 0.149 for all data.

Calculations. All calculations were performed using the Gaussian 03 package.[15] Structures were initially optimized using standard methods with the STO-3G* basis sets for C, B, P, S, and H and with the LANL2DZ basis set for the rhodium atom. The final optimizations, including frequency analyses to confirm the true minima, together with GIAO nuclear-shielding calculations, were performed using B3LYP methodology, with the 6-31G* and LANL2DZ basis sets. The GIAO nuclear shielding calculations were performed on the final optimized geometries, and computed ^{11}B shielding values were related to chemical shifts by comparison with the computed value for B_2H_6, which was taken to be $\delta(^{11}B)$ +16.6 ppm relative to the $BF_3(OEt_2)$ = 0.0 ppm standard.

Kinetic Analysis. The kinetics of the substitution reaction between **2** and PMe_2Ph were measured in 0.02 M solutions of the hydridorhodathiaborane in CD_2Cl_2. The decay of the hydride complex resonance was monitored by ^1H NMR spectroscopy (Tables S4 and S5). The integrals were normalized relative to the solvent peak that was used as an internal standard.

The activation parameters, $\Delta H^{\ddagger}$ and $\Delta S^{\ddagger}$, were obtained from a linear least-squares fit of $\ln(k/T)$ vs $1/T$ (Eyring equation). Errors were computed by published methods.[16] The error in temperature was assumed to be 1 K; the error in k_{obs} was estimated as 10%.

*Synthesis of [8,8,8-(H)(PMePh$_2$)$_2$-9-(Py)-nido-8,7-RhSB$_9$H$_9$] (****4****).* A 82.7 mg (0.083 mmol) amount of **2**, placed in a Schlenk tube, was dissolved in 15 mL of CH_2Cl_2 under an atmosphere of argon. Three equivalents of $PMePh_2$ (58.06 mL, 0.29 mmol) was added, and the resulting solution was stirred for 4 h. Solvent was reduced in volume, and hexane added to form a yellow precipitate, which was separated by decantation, washed with hexane, and dried under vacuum. The resulting yellow product was characterized as **4** (39.2 mg, 0.054 mmol, 56%). IR (ATR): ν_{max}/cm^{-1} 2512 m (BH), 2011 m (RhH). $^{11}B\{^1H\}$ NMR (160 MHz; $CDCl_3$; 298 K): δ 12.2 (1B, br, BH), 6.0 (1B, d, $^1J_{B-H}$ = 112 Hz, BH), 1.9 (1B, br, BH), −0.5 (1B, br, BH), −4.5 (1B, br, BH), −10.1 (1B, d, $^1J_{B-H}$ = 142 Hz, BH), −19.7 (1B, br, BH), −27.1 (2B, d, $^1J_{B-H}$ = 142 Hz, BH). $^1H\{^{11}B\}$ NMR (300 MHz; CD_2Cl_2; 298 K): δ 8.17 (2H, m, Py), 7.85 (1H, m, Py), 7.54 (1H, m, Py), 7.45 (1H, m, Py), 7.32−6.85 (20H, aromatic, 2PMe*Ph*$_2$), 3.86 (1H, br, BH), 3.46 (1H, br, BH), 2.86 (1H, br, BH), 2.39 (1H, br, BH), 1.84 (1H, br, BH), 1.83 (3H, d, $^2J_{P-H}$ = 7.1 Hz, P*Me*Ph$_2$), 1.64 (3H, d, $^2J_{P-H}$ = 7.0 Hz, P*Me*Ph$_2$), 1.39 (1H, s, BH), 1.32 (1H, s, BH), 0.92 (1H, s, BH), −1.34 (1H, s, BHB), −12.54 (1H, q, $^1J_{Rh-H} \approx {}^2J_{P-H}$ = 13 Hz, Rh−H). $^{31}P\{^1H\}$ NMR (161 MHz; $CDCl_3$; 223 K): δ 17.4 (1P, dd, $^1J_{Rh-P}$ = 104 Hz, $^2J_{PP}$ too broad to be resolved), 12.6 (1P, dd, $^1J_{Rh-P}$ = 128 Hz, $^2J_{P-P}$ = 18 Hz). MS m/z (MALDI): 520 [M^+ − (PPh_2Me + 2H), isotope envelope; $PC_{18}H_{26}RhSB_9N$ requires 520; $C_{11}H_{33}B_9NP_2RhS$ requires 722].

*[8,8,8-(H)(L)(PPh$_3$)-9-(Py)-nido-8,7-RhSB$_9$H$_9$] where L = PMe$_2$Ph (****5****), PMe$_3$ (****6****).* *Compound* ***5****.* The procedure was the same as for **4**, using 38.5 mg (0.045 mmol) of **2** and two equivalents of PMe_2Ph (19.4 μL, 0.14 mmol) and stirring the resulting solution for 15 min. The resulting orange product was characterized as **5** (30.5 mg, 0.042 mmol, 93%), which is a mixture of two isomers, **5a** and **5b**. Both isomers appear to exhibit the same $^{11}B\{^1H\}$ NMR (160 MHz; $CDCl_3$; 298 K): δ 12.1 (1B, s, BN), 4.3 (1B, br BH), −0.9 (2B, d, $^1J_{B-H}$ = 102 Hz, BH), −4.9 (1B, br, BH), −9.6 (1B, d BH), −21.4 (1B, br, BH), −25.9 (1B, d, $^1J_{B-H}$ = 159 Hz, BH), −27.6 (1B, d, $^1J_{B-H}$ = 142 Hz, BH); similarly, the directly boron-bound proton resonances were indistinguishable for the isomers: $^1H\{^{11}B\}$ NMR (300 MHz; CD_2Cl_2; 298 K): δ 3.86 (1H, s, BH), 3.48 (1H, s, BH), 3.27 (1H, s, BH), 2.68 (1H, s, BH), 1.73 (1H, s, BH), 1.43 (1H, s, BH), 1.29 (1H, s, BH), 0.83 (1H, s, BH), −1.27 (1H, s, BHB). MS m/z (MALDI): 721 [(M^+ − H), isotope envelope;

dx.doi.org/10.1021/om2009205 | *Organometallics* 2012, 31, 2986−2995

$P_2C_{31}H_{41}RhSB_9N$ requires 722], 582 [(M^+ − PMe_2Ph − 2H), isotope envelope].

Additional NMR data for ***5a****:* $^1H\{^{11}B\}$ NMR (400 MHz, CD_2Cl_2): δ +1.53 (3H, doublet, $^2J_{H-P}$ = 7.5 Hz, P*Me*$_2$Ph), +1.36 (3H, doublet, $^2J_{H-P}$ = 7.5 Hz, P*Me*$_2$Ph), −13.02 (1H, q, $^1J_{H-Rh} \approx {}^2J_{H-P}$ = 20 Hz, Rh−H). $^{31}P\{^1H\}$ NMR (162 MHz; CD_2Cl_2; 223 K): δ +35.2 (1P, dd, $^1J_{P-Rh}$ = 128 Hz, $^2J_{PP}$ = 28 Hz, PPh_3), −2.9 (1P, dd, $^1J_{P-Rh}$ = 105 Hz, $^2J_{P-P}$ = 27 Hz, PMe_2Ph).

Additional NMR data for ***5b****:* $^1H\{^{11}B\}$ NMR (300 MHz, $CDCl_3$): δ +1.44 (3H, d, $^2J_{H-P}$ = 7.4 Hz, P*Me*$_2$Ph), +1.01 (3H, d, $^2J_{H-P}$ = 7.7 Hz, P*Me*$_2$Ph), −12.78 (1H, q, $^1J_{H-Rh} \approx {}^2J_{H-P}$ = 22 Hz, Rh−H). $^{31}P\{^1H\}$ NMR (162 MHz; CD_2Cl_2; 223 K): δ +39.2 (1P, dd, $^1J_{P-Rh}$ = 108 Hz, $^2J_{P-P}$ = 19 Hz, PPh_3), −2.1 (1P, dd, $^1J_{P-Rh}$ = 128 Hz, $^2J_{P-P}$ = 19 Hz, PMe_2Ph).

Compound ***6****.* Following the same synthetic steps described for compounds **4** and **5**, 76.1 mg (0.069 mmol) of **2** was treated with two equivalents of PMe_3 (18.5 mL, 0.18 mmol). Yield: yellow product, 0.023 g (0.048 mmol, 54%). Anal. Calcd for $C_{26}H_{39}B_9NP_2RhS$: C, 47.33; H, 5.96; N, 2.12; S, 4.86. Found: C, 47.07; H, 5.88; N, 1.45; S, 3.95. IR (ATR): ν_{max}/cm^{-1} 2910 m (BH), 2112 m (RhH). $^{31}P\{^1H\}$ NMR (161 MHz; CD_2Cl_2; 223 K): δ 36.9 (dd, $^1J_{Rh-P}$ = 129 Hz, $^2J_{P-P}$ = 30 Hz, PPh_3), −12.9 (br d, $^1J_{P-Rh}$ = 103 Hz, PMe_3). MS *m*/*z* (MALDI): 409 [M^+ − (PPh_3 + 1H), isotope envelope; $PC_8H_{33}RhSB_9N$].

Synthesis of [8,8,8-(H)(PMe$_2$Ph)$_2$-9-(Py)-*nido*-8,7-RhSB$_9$H$_9$] (7). **2** (12 mg, 0.014 mmol) was treated with PMe_2Ph (7.8 mg, 8 mL, 0.057 mmol) in 10 mL of CH_2Cl_2. The resulting solution was stirred under an atmosphere of argon for 2.5 h. Solvent was evaporated, and the solid subjected to NMR studies in CD_2Cl_2. The NMR spectra showed that the product of the reaction contained the isomers **5a** and **5b** together with the bis-PMe_2Ph-substituted cluster **7** in a 1:1:2 ratio. Isolation of compound **7** was not possible due to its instability toward dehydrogenation; therefore, the characterization of **7** was carried out *in situ* by NMR spectroscopy. $^{31}P\{^1H\}$ NMR (161 MHz; CD_2Cl_2; 298 K): δ 3.2 (d, $^1J_{Rh-P}$ = 77 Hz, P_B *trans* to B(9)), −1.8 (dd, $^1J_{Rh-P}$ = 124 Hz, $^2J_{P-P}$ = 24 Hz, P_A *trans* to B(3)−B(4) edge).

Synthesis of [1,1-(PPh$_3$)(PMe$_2$Ph)-3-(Py)-*closo*-1,2-RhSB$_9$H$_8$] (9). A 5.9 mg (0.0082 mmol) amount of a mixture of isomers **5a** and **5b** was dissolved in CD_2Cl_2 in an NMR tube and heated at 70 °C for 3 h. Solvent was reduced in volume, and hexane added to form a yellow precipitate, which was separated by decantation, washed with hexane, and dried under vacuum. The resulting red product was characterized as **9** (4.2 mg, 0.059 mol, 72%). $^{31}P\{^1H\}$ NMR (161 MHz; $CDCl_3$; 223 K): δ 50.7 (dd, $^1J_{RhP}$ = 155 Hz, $^2J_{PP}$ = 30 Hz, PPh_3), −6.2 (dd, $^1J_{RhP}$ = 138 Hz, $^2J_{PP}$ = 32 Hz, PMe_2Ph).

Synthesis of [1,1-(PPh$_3$)(PMe$_3$)-3-(Py)-*closo*-1,2-RhSB$_9$H$_8$] (10). A 10 mg (0.021 mmol) sample of **6**, placed in an Schlenk tube, was dissolved in CH_2Cl_2 and heated to reflux temperature under an atmosphere of argon for 3 h. Solvent was reduced in volume, and hexane added to form a yellow precipitate, which was separated by decantation, washed with hexane, and dried under vacuum. The resulting yellow product was characterized as **10** (6.9 mg, 0.015 mmol, 69%). $^{31}P\{^1H\}$ NMR (161 MHz; $CDCl_3$; 300 K) ordered as δ_P [DFT-calcd δ_P]: 49.2 [67.7] (dd, $^1J_{Rh-P}$ = 157 Hz, $^2J_{P-P}$ = 29 Hz, PPh_3), −15.4 [−3.2] (1P, dd, $^1J_{Rh-P}$ = 146 Hz, PMe_3). Anal. Calcd for $C_{26}H_{37}B_9NP_2RhS$: C, 47.47; H, 5.67; N, 2.13; S, 4.87. Found: C, 47.07; H, 5.88; N, 2.39; S, 3.77.

Synthesis of [1,1-(PMe$_2$Ph)$_2$-3-(Py)-*closo*-1,2-RhSB$_9$H$_8$] (11). A Schlenk tube was charged with the mixture of isomers **5** (10.1 mg, 0.012 mmoL). The mixture of hydridorhodathiaboranes was dissolved in 10 mL of CH_2Cl_2, and then PMe_2Ph (2.5 μL, 0.024 mmol) was added under an argon atmosphere. The resulting solution was heated at reflux in an argon atmosphere for 12 h. Solvent was evaporated, and the red residue crystallized in CH_2Cl_2/hexane to give 6.0 mg of compound **11** (0.010 mmol, 84%). $^{31}P\{^1H\}$ NMR (161 MHz; CD_2Cl_3; 300 K): δ 2.9 (d, $^1J_{Rh-P}$ = 140 Hz). Anal. Calcd for $C_{21}H_{35}B_9NP_2RhS$: C, 42.34; H, 5.92; N, 2.35; S, 5.38. Found: C, 41.88; H, 5.87; N, 2.18; S, 4.70. MS *m*/*z* (MALDI): 596 (M^+, isotope envelope; $C_{21}H_{35}B_9NP_2RhS$ requires 596).

Synthesis of [1,1-(PMe$_3$)$_2$-3-(Py)-*closo*-1,2-RhSB$_9$H$_8$] (12). A Schlenk tube was charged with **2** (112.8 mg, 0.1333 mmol). The rhodathiaborane was dissolved in 10 mL of CH_2Cl_2, and then three equivalents of PMe_3 (399.9 μL, 0.399 mmol) was added under an argon atmosphere. The resulting solution was heated at 70 °C in an argon atmosphere for 12 h. Then, solvent was evaporated, and the resulting solid crystallized in CH_2Cl_2/hexane, affording **12**. Yield: 56.1 mg, 0.1189 mmol, 89.2%. $^{31}P\{^1H\}$ NMR (121 MHz; $CDCl_3$; 300 K): δ −9.3 (2P, d, $^1J_{Rh-P}$ = 147 Hz). Anal. Calcd for $C_{11}H_{31}B_9NP_2RhS$: C, 28.02; H, 6.62; N, 2.97; S, 6.80. Found: C, 27.86; H, 6.59; N, 2.86; S, 6.48.

Synthesis of [1,1-(CO)(PMe$_2$Ph)-3-(Py)-*closo*-1,2-RhSB$_9$H$_8$] (16). A 51.02 mg portion of the isomer mixture of **5** (0.0707 mmol) was loaded in a Schlenk tube and dissolved in 10 mL of CH_2Cl_2. A balloon filled with CO(g) was attached to the Schlenk tube; the system was then cooled in liquid nitrogen and evacuated under vacuum. The system was exposed to the carbon monoxide atmosphere created upon opening of the balloon, and the reaction was stirred overnight at room temperature. The solvent was evaporated under vacuum, and the red solid studied by NMR. The data demonstrated formation of the PPh_3-ligated *closo*-rhodathiaborane **14** and the CO-ligated analogue **15** in a 1:4 ratio, which results in a yield of 53% for **16** (nonisolated, calculated from the NMR data). NMR data of **15**: IR(ATR): ν_{max}/cm^{-1} 2507 vs (BH), 1969 vs (CO), 1620 m, 1482 m, 1458 m, 1434 m, 1259 m, 1093 m, 1006 s, 905 s, 799 m, 682 s, 524 m, 488 m. $^{31}P\{^1H\}$ NMR (202 MHz; $CDCl_3$; 300 K): δ 1.9 (d, $^1J_{Rh-P}$ = 129 Hz, PMe_2Ph).

Synthesis of [1,1-(CO)(PMe$_3$)-3-(Py)-*closo*-1,2-RhSB$_9$H$_8$] (17). An orange solution of **6** (10 mg, 0.015 mmol) in 2 mL of CD_2Cl_2 was stirred under an atmosphere of CO(g) at room temperature for 15 min, during which time the initial bright orange solution became yellow. The final mixture was washed repeatedly with hexane to give 5.9 mg of **17** (0.014 mmol, 92%). IR (ATR): ν_{max}/cm^{-1} 2521 s (BH), 2475 s (BH), 1979 vs (CO), 1620 m, 1480 m, 1457 m, 1434 m, 1156 m, 1091 m, 1006 m, 933 m, 799 m, 681 m. $^{11}B\{^1H\}$ NMR (160 MHz; CD_2Cl_2; 298 K): δ 55.0 (1B, s, B-py), 27.4 (1B, d, $^1J_{B-H}$ = 129 Hz, BH), 0.7 (1B, br, BH), −1.8 (1B, d, $^1J_{B-H}$ = 120 Hz, BH), −14.1 (1B, br, BH), −25.8 (1B, br, BH), −32.3 (1B, d, $^1J_{B-H}$ = 149 Hz, BH), −33.8 (1B, d, $^1J_{B-H}$ = 146 Hz, BH). ^1H NMR (300 MHz; CD_2Cl_2; 300 K): δ 9.41 (2H, d, *J* = 5.6 Hz, Py), 8.26 (1H, m, Py), 7.82 (2H, m, Py), 4.40 (1H, s, BH), 2.51 (1H, s, BH), 2.17 (1H, s, BH), 1.83 (1H, s, BH), +1.35 (3H, d, $^2J_{P-H}$ = 10.3 Hz, P*Me*$_3$), 0.38 (1H, s, BH), 0.32 (1H, s, BH), 0.05 (1H, s, BH), 0.02 (1H, s, BH). $^{31}P\{^1H\}$ NMR (202 MHz; CD_2Cl_2; 300 K): δ −6.1 (d, $^1J_{Rh-P}$ = 137 Hz, PMe_3); *m*/*z* (MALDI$^-$) 421 (M − 4H; isotope envelop; $PC_9H_{22}ORhSB_9N$ requires 425).

Reactions of 9−12, 16, and 17 with H$_2$(g). In a typical reaction, around 10 mg (0.016 mmol) of the *closo*-rhodathiaboranes was placed in a screw-capped NMR tube and dissolved in 0.6 mL of CD_2Cl_2. The NMR tube was cooled in liquid nitrogen, evacuated, and then filled with H_2. The samples were monitored at different intervals overnight by ^1H NMR spectroscopy, without evidence of changes in the spectra.

Reactions of 4−6 with C$_2$H$_4$. In a Schlenk tube, around 10 mg of the hydridorhodathiaboranes **4**−**6** was dissolved in CH_2Cl_2 (∼8 mL). A balloon filled with C_2H_4 was attached to the Schlenk tube; the system was then cooled in liquid nitrogen and evacuated under vacuum. The hydrorhodathiaborane solutions were exposed to the ethylene atmosphere created upon the opening of the balloon, and the reaction was stirred overnight at room temperature. In the case of compound **4**, the NMR data demonstrated that there was no reaction with the olefin. In the case of **6**, however, there was formation of the *closo*-derivative **10**. In the same conditions, a mixture of the isomers **5a** and **5b** leads to the formation of the bis-PMe_2Ph derivative **11**.

Compound ***6*** *with Ethylene.* Alternatively, the reaction with compound **6** (5.5 mg, 0.0083 mmol, in 0.4 mL of CD_2Cl_2) was carried out in a screw-capped NMR tube, which was exposed to 1.5 bar of ethylene. After 3 days, the ^1H NMR spectrum at room temperature exhibits two broad multiplets at +2.27 and +2.05 ppm, which correspond to the previously reported ethylene-ligated rhodathiaborane, **13**. In addition, there are two broad multiplets of higher intensity at +2.38 and +2.16 ppm, which can be assigned to the rhodium-bound ethylene ligand of the PMe_3-ligated analogue [1,1-(PMe_3)(η^2-C_2H_4)-3-(Py)-*closo*-1,2-$RhSB_9H_8$] (**15**). At lower temperatures, the two

dx.doi.org/10.1021/om2009205 | *Organometallics* 2012, 31, 2986−2995

signals of the ethylene ligand in **15** split into four peaks, which coalesce in pairs over the range 196−300 K to give a free energy for the rotation of the ethylene ligand of ΔG_{273} = 53 kJ/mol (vs ΔG_{252} = 49 kJ/mol for **13**;[2b] see Supporting Information, Figure S17).

*[1,1-(PMe$_3$)(η^2-C$_2$H$_4$)-3-(Py)-closo-1,2-RhSB$_9$H$_8$] (**15**)*. NMR data were assigned from a mixture that contains **10** (major), **13** (minor), and **15** (medium). ^{11}B{^{1}H} NMR (160 MHz; CD_2Cl_2; 298 K): δ 54.5 (1B, s, B-py), 24.9 (1B, b, BH), 0.9 (1B, b, BH), −1.1 (1B, b, BH), −20.5 (1B, b, BH), −27.6 (1B, b, BH), 30.5 (1B, b, BH), −31.7 (1B, b, BH). ^{1}H{^{11}B} NMR (300 MHz; CD_2Cl_2; 298K): δ 4.37 (1H, s, BH), +1.18 (3H, d, $^2J_{H-P}$ = 10.2 Hz, P-CH$_3$), 0.46 (1H, s, BH), 0.01 (1B, s, BH), −0.57 (1B, s, BH). ^{31}P{^{1}H} NMR (161 MHz; CD_2Cl_2; 300 K): δ −5.1 (1P, d, $^1J_{P-Rh}$ = 134 Hz, PMe$_3$).

Regarding the ^{11}B and ^{1}H NMR data, the assignments are tentative since there is overlapping of signals with the other two rhodathiaboranes, **10** and **13**. The ^{31}P{^{1}H} data, however, can be unambiguously assigned.

In a higher scale, 50.2 mg (0.059 mmol) of **6** was placed in a screw-capped Schlenk tube and dissolved in 25 mL of CH_2Cl_2. The resulting solution was frozen at the liquid nitrogen temperature, and the system evacuated under vacuum and then exposed to 1.5 bar of ethylene. After 7 days of stirring at room temperature, the solvent was evaporated to dryness and applied to preparative TLC plates. The chromatogram was developed using CH_2Cl_2/hexane (3:1) as mobile phase to give broad yellow (R_f = 0.33) and red (R_f = 0.13) bands. The former was a mixture of compounds **13** (1.71 mg, 0.0028 mmol, 5%) and **15** (4.28 mg, 0.010 mmol, 17%) in a 1:4 ratio, whereas the second was compound **10** (12 mg, 0.018 mmol, 31%). It was found that compounds **13** and **15** decompose largely on the plates; thus, a second preparative TLC plate resulted in the loss of both species.

In the same conditions, using screw-capped NMR and Schlenk tubes and 1.5 bar of ethylene, the mixture of isomers **5** afforded compound **11** as the major component and small amounts of the ethylene-ligated cluster **13**. However, we did not detect the ethylene-ligated PMe$_2$Ph counterpart.

■ ASSOCIATED CONTENT

Ⓢ Supporting Information

^{31}P{^{1}H} NMR spectra at different temperatures of compounds **2** and **6**; NMR spectra of the reactions of **2** with PMe$_3$, PMe$_2$Ph, and PMePh$_2$ at different temperatures; series of ^{1}H−^{31}P HSQC, ^{31}P{^{1}H}, and ^{1}H NMR spectra of samples that contain mixtures of **5a**, **5b**, and **7**; tables of the kinetics studies; the Eyring plot; ORTEP-type picture for compound **11**; experimental and DFT-calculated coordinates and energy for **6** and **10**; CIF files for **4**, **10**, and **11**. This material is available free of charge via the Internet at http://pubs.acs.org.

■ AUTHOR INFORMATION

Corresponding Author

*E-mail: rmacías@unizar.es.

Notes

The authors declare no competing financial interest.

■ ACKNOWLEDGMENTS

We acknowledge the Spanish Ministry of Science and Innovation (CTQ2009-10132, CONSOLIDER INGENIO, CSD2009-00050, MULTICAT, and CSD2006-0015, Crystallization Factory) for support of this work. B.C. thanks the "Diputación General de Aragón" for a predoctoral scholarship. P.G.O. acknowledges financial support from the CSIC *JAE-DOC* program, contract co-funded by the ESF. We also thank ESRF BM16 beamline staff for their support of data acquisition of **4**.

■ REFERENCES

(1) Ferguson, G.; Jennings, M. C.; Lough, A. J.; Coughlan, S.; Spalding, T. R.; Kennedy, J. D.; Fontaine, X. L. R.; Stibr, B. *J. Chem. Soc., Chem. Commun.* **1990**, 891.

(2) (a) Álvarez, A.; Macías, R.; Fabra, M. J.; Lahoz, F. J.; Oro, L. A. *J. Am. Chem. Soc.* **2008**, *130*, 2148. (b) Alvarez, A.; Macias, R.; Bould, J.; Fabra, M. J.; Lahoz, F. J.; Oro, L. A. *J. Am. Chem. Soc.* **2008**, *130*, 11455. (c) Alvarez, A.; Macias, R.; Bould, J.; Cunchillos, C.; Lahoz, F. J.; Oro, L. A. *Chem.—Eur. J.* **2009**, *15*, 5428.

(3) Calvo, B.; Kess, M.; Macias, R.; Cunchillos, C.; Lahoz, F. J.; Kennedy, J. D.; Oro, L. A. *Dalton Trans.* **2011**, *40*, 6555.

(4) (a) Wade, K. *Inorg. Nucl. Chem. Lett.* **1972**, *8*, 559. (b) Wade, K. *Adv. Inorg. Chem. Radiochem.* **1976**, *18*, 1. (c) Mingos, D. M. P. *Nature (London), Phys. Sci.* **1972**, *99*, 236. (d) Mingos, D. M. P.; Wales, D. J. *Introduction to Cluster Chemistry*; Prentice Hall: London, 1990.

(5) (a) Kennedy, J. D. In *The Borane-Carborane-Carbocation Continuum*; Casanova, J., Ed.; Wiley: New York, 1998. (b) Macías, R.; Bould, J.; Holub, J.; Kennedy, J. D.; Štibr, B.; Thornton-Pett, M. *Dalton Trans.* **2007**, 2885. (c) Murphy, M. P.; Spalding, T. R.; Cowey, C.; Kennedy, J. D.; Thornton-Pett, M.; Holub, J. *J. Organomet. Chem.* **1998**, *550*, 151.

(6) Ferguson, G.; Lough, A. L.; Coughlan, S.; Spalding, T. R. *Acta Crystallogr., Sect. C: Cryst. Struct. Commun.* **1992**, *C48*, 440.

(7) Beall, H.; Bushweller, C. H.; Dewkett, W. J.; Grace, M. *J. Am. Chem. Soc.* **1970**, *92*, 3484.

(8) Macías, R.; Rath, N. P.; Barton, L. *Organometallics* **1999**, *18*, 3637.

(9) Otwinowski, Z.; Minor, W. In *Methods in Enzymology*; Carter, J. R. M. S. C. W., Ed.; Academic Press: New York, 1997; Vol. *276*.

(10) Blessing, R. H. *Acta Crystallogr.* **1995**, *A51*, 33.

(11) Sheldrick, G. M. *SHELXS-86*; University of Göttingen: Göttingen, Germany, 1997.

(12) Sheldrick, G. M. *Acta Crystallogr.* **2008**, *A64*, 112.

(13) Farrugia, L. J. *J. Appl. Crystallogr.* **1999**, *32*, 837.

(14) Spek, A. L. *J. Appl. Crystallogr.* **2003**, *36*, 7.

(15) Frisch, M. J.; Trucks, G. W.; Schlegel, H. B.; Scuseria, G. E.; Robb, M. A.; Cheeseman, J. R.; Montgomery, J. A., Jr.; Vreven, T.; Kudin, K. N.; Burant, J. C.; J. M.Millam; Iyengar, S. S.; Tomasi, J.; Barone, V.; Mennucci, B.; Cossi, M.; Scalmani, G.; Rega, N.; Petersson, G. A.; Nakatsuji, H.; Hada, M.; Ehara, M.; Toyota, K.; Fukuda, R.; Hasegawa, J.; Ishida, M.; Nakajima, T.; Honda, Y.; Kitao, O.; Nakai, H.; Klene, M.; Li, X.; Knox, J. E.; Hratchian, H. P.; Cross, J. B.; Bakken, V.; Adamo, C.; Jaramillo, J.; ; Gomperts, R.; Stratmann, R. E.; Yazyev, O.; Austin, A. J.; Cammi, R.; Pomelli, C.; Ochterski, J.; Ayala, P. Y.; Morokuma, K.; Voth, G. A.; Salvador, P.; Dannenberg, J. J.; Zakrzewski, V. G.; Dapprich, S.; Daniels, A. D.; Strain, M. C.; Farkas, O.; Malick, D. K.; Rabuck, A. D.; Raghavachari, K.; Foresman, J. B.; Ortiz, J. V.; Cui, Q.; Baboul, A. G.; Clifford, S.; Cioslowski, J.; Stefanov, B. B.; Liu, G.; Liashenko, A.; Piskorz, P.; Komaromi, I.; L.Martin, R.; Fox, D. J.; Keith, T.; Al-Laham, M. A.; Peng, C. Y.; Nanayakkara, A.; Challacombe, M.; Gill, P. M. W.; Johnson, B. G.; Chen, W.; Wong, M. W.; Gonzalez, C.; Pople, J. A.*Gaussian 03*; Gaussian, Inc.: Wallingford, CT, 2004.

(16) Morse, P. M.; Spencer, M. D.; Wilson, S. R.; Girolami, G. S. *Organometallics* **1994**, *13*, 1646.